DISCRETE AND CONTINUOUS
DYNAMICAL SYSTEMS
Volume **29**, Number **4**, April **2011**

doi:10.3934/dcds.2011.29.1367

pp. **1367–1391**

A BIHARMONIC-MODIFIED FORWARD TIME STEPPING METHOD FOR FOURTH ORDER NONLINEAR DIFFUSION EQUATIONS

Andrea L. Bertozzi

Department of Mathematics, University of California
Los Angeles, CA, 90095-1555, USA

Ning Ju

Department of Mathematics, 401 Mathematical Sciences, Oklahoma State University
Stillwater, OK 74078, USA

Hsiang-Wei Lu

Department of Mechanical Engineering, University of California
Los Angeles, CA, 90095-1555, USA

Abstract. We consider a class of splitting schemes for fourth order nonlinear diffusion equations. Standard backward-time differencing requires the solution of a higher order elliptic problem, which can be both computationally expensive and work-intensive to code, in higher space dimensions. Recent papers in the literature provide computational evidence that a biharmonic-modified, forward time-stepping method, can provide good results for these problems. We provide a theoretical explanation of the results. For a basic nonlinear 'thin film' type equation we prove H^1 stability of the method given very simple boundedness constraints of the numerical solution. For a more general class of long-wave unstable problems, we prove stability and convergence, using only constraints on the smooth solution. Computational examples include both the model of 'thin film' type problems and a quantitative model for electrowetting in a Hele-Shaw cell (Lu *et al* J. Fluid Mech. 2007). The methods considered here are related to 'convexity splitting' methods for gradient flows with nonconvex energies.

1. **Introduction.**

Higher order PDEs arise in a number of problems in physics, biology, and image processing. Many of these applications involve curvature effects that lead to very stiff differential equations. With the development of high performance computing, it is now possible to solve these problems computationally in a reasonable time. A number of papers in the recent literature address the problem of efficient numerical schemes for such equations.

In this paper we focus on a class of PDEs that arise in the study of thin films and phase field models [20]. The general form is

$$u_t = \nabla \cdot (f(u)\nabla w)\,, \tag{1.1}$$

$$w = -\gamma\Delta u + \varphi(u), \tag{1.2}$$

2000 *Mathematics Subject Classification.* 65M06, 65M12, 65M70.

Key words and phrases. Fourth order equations, convex splitting.

This research is supported by ONR grant N000140710431, UC Lab Fees Research grant 09-LR-04-116741-BERA, and NSF grants DMS-0244498 and ACI-0321917.

where f is non-negative, $u > 0$, and both f and φ are smooth. For simplicity of presentation, we impose periodic boundary conditions. However, many of our results are still valid for some other typical boundary conditions as well and we omit detailed discussion here.

In the following, we take $\gamma = 1$. Then, one can write the model equivalently as

$$u_t = -\nabla \cdot (f(u)\nabla\Delta u) + \nabla \cdot (f(u)\nabla\varphi(u)), \tag{1.3}$$

or

$$u_t = -\nabla \cdot (f(u)\nabla\Delta u) + \nabla \cdot (g(u)\nabla u), \tag{1.4}$$

where

$$g(u) := f(u)\varphi'(u). \tag{1.5}$$

Examples in the literature include the thin film equations [42, 30, 29, 40, 35, 33, 34, 36, 18, 46, 48] in which f is typically u^3 plus a possible lower order polynomial. In degenerate Cahn-Hilliard equations, f is of polynomial form, for example u or $u(1-u)$ [20, 51].

For simplicity of discussion, we assume periodic boundary conditions. However, we wish to point out that many results obtained here are valid for other boundary conditions as well upon proper slight modifications where necessary.

If we denote $\varphi(u) = \psi'(u)$, then

$$\psi''(u) = \frac{g(u)}{f(u)},$$

and there is a Lyapunov functional for the equations (1.1)-(1.2) as follows.

$$\frac{d}{dt}\int_\Omega \left(\frac{\gamma}{2}|\nabla u|^2 + \psi(u) + cu\right)dx \leqslant 0,$$

where c is any constant. Notice that conservation of mass always holds:

$$\frac{d}{dt}\int_\Omega u(x,t)dx \equiv 0.$$

When ψ is positive, one can obtain an a priori H^1 bound. When ψ is negative, finite-time blowup is possible [10]. Here we consider the case where ψ may be either positive or negative, or may change sign.

Numerical methods for such problems have been the subject of ongoing study in the literature. Barrett, Blowey and Garke [5, 6] prove convergence of finite element methods for the class of equations. In [5] they prove convergence for the pure fourth order problem (with $\varphi \equiv 0$) with a semi-implicit time-step in which f is evaluated at the old time level. In [6] they include the φ term and perform semi-implicit time-stepping as in [5] for the highest order term and a convexity splitting for the lower order term. Zhornitskaya and Bertozzi [52] introduce and prove convergence of positivity preserving finite difference and finite element schemes for ([32]) with $\varphi = 0$; their paper considers the spatial discretization only and shows that a special choice of treatment of the nonlinearity yields schemes that dissipate a discrete form of the entropy $\int_\Omega G(u)$, $G'' = f$, as well as the well-known H^1 energy $\int_\Omega |\nabla u|^2 dx$. Grün and Rumpf [32] consider related finite element schemes that are nonnegativity preserving. Moreover, they introduce analysis for a backward Euler timestepping method, leading to solution of the implicit problem

$$U_{n+1} - U_n = -\Delta t \nabla \cdot (f(U_{n+1})\nabla\Delta U_{n+1})$$

for a suitable spatial discretization of the differential operators. They solve this implicit problem using iterative methods that require both good preconditioners and a good initial guess of solutions for the method. Even with good initial guess, solving the problem in 2D (or higher dimensional cases for other physical problems) can still require a large number of iterations (tens or hundreds) at each time-step.

While much work has been done on finite element methods, others have focused attention on finite difference methods that take advantage of easy to implement fast methods for subproblems. One such example are the Alternating Direction Implicit (ADI) methods proposed by Witelski and Bowen [50]. These have the advantage of solving repeated implicit steps in one space dimension, thus taking advantage of inexpensive solvers for higher order problems on the line. In this paper we consider another class of finite difference methods. These are explicit time stepping methods, which would ordinarily be only conditionally stable and quite stiff. However, by modifying the method with a semi-implicit biharmonic operator, we are able to design methods that can be both unconditionally stable and easy to implement. Such methods were proposed for diffuse interface equations for Hele-Shaw flow [25, 39]. For the class of equations we consider here, the scheme takes on the form

$$\begin{aligned}\frac{U_{n+1}-U_n}{\Delta t} &+ M_1\Delta^2 U_{n+1}\\ &= \nabla\cdot\left[(M_1 - f(U_n))\nabla\Delta U_n\right] + \nabla\cdot\left(g(U_n)\nabla U_n\right),\end{aligned} \tag{1.6}$$

where M_1 can be chosen as a number no less than $\max_n |f(U_n)|$. For example, one can choose simply $M_1 > 0$ such that

$$\|f(u(\cdot,\cdot))\|_\infty \leqslant M_1 < +\infty,$$

where the norm $\|\cdot\|_\infty$ denotes the maximum norm. We refer to schem (1.6) as a biharmonic modified forward time-stepping method because the terms for the equation of interest are all evaluated at the old time. However there is one additional term added and subtracted, which has a pure biharmonic operator. This method is similar in spirit to the Laplace-modified forward time-stepping method introduced by Douglas and Dupont in [16]. They consider second order nonlinear diffusion equations with a related temporal splitting of the form

$$\frac{U_{n+1}-U_n}{\Delta t} + \Delta U_{n+1} = \nabla\cdot\left[(1-g(U_n))\nabla U_n\right], \tag{1.7}$$

for the case of equation (1.3) with f term zeroed out.

Schemes of the form (1.6) have also been used to solve higher order, level-set based curvature evolution equations [31, 47]. The computational advantage to using a scheme of the form (1.6) or (1.7) is that the implicit calculation involves only the biharmonic operator (or Laplace operator in the case of 1.7). While the original Douglas-Dupont paper combines the method with alternating direction implicit time stepping for the Laplace problem, we note that recent implementations of such schemes on square grids use spectral solvers for the implicit calculation, thus taking advantage of the Fast Fourier transform. The idea considered here has some relation to the convexity splitting methods recently studied for variational problems with non-convex energies, such as the Cahn-Hilliard and Allen-Cahn equations. See [21, 49] for a discussion of these problems. See also [1] and [19]. Our paper differs most from those in that we consider a splitting of the highest order term in the equation in order to treat the nonlinearity explicitly.

This paper is organized as follows: Section 2 reviews what is known about solutions of the PDE and of the proposed scheme. For simplicity we consider analysis of the timestepping problem, with continuous spatial derivatives. It is straightforward to extend the results to finite difference or finite element operators in space. Section 3 contains the rigorous part of the paper. Section 3.1 discusses consistency of the scheme under the assumption of sufficient regularity of the PDE solution. Section 3.2 proves our key boundedness result for the scheme. Section 3.3 proves convergence of the scheme. Section 4 shows some numerical simulations and discussion of empirical convergence results and modified equation analysis.

We note that the finite difference scheme and convergence estimates described here have some features in common with the works of [2], [4] and [3], and the similarity necessitates some discussion. Since these three earlier papers use some common techniques, we focus on the comparison of our work with that of [4]. We note that a similar method was used as well in the computations performed in [25] in the finite difference setting.

In [4], a version of bi-harmonic modification was proposed of the form

$$\begin{aligned}\frac{U_{n+1}-U_n}{\Delta t}+&M_1\Delta\left[\Delta U_{n+1}-\varphi(U_{n+1})\right]\\ &=\nabla\cdot\left[(M_1-f(U_n))\nabla(\Delta U_n-\varphi(U_n))\right],\end{aligned} \tag{1.8}$$

where M_1 is chosen similarly as for (1.6). The main difference is that this scheme is *nonlinear* in U_{n+1}, while our scheme is *linear* in U_{n+1}. Notice the extra third term on the left hand side of (1.8). Moreover, they use a finite element method for the spatial discretization. Note that the relationship between the terms $M_1\Delta^2 U_{n+1}$ and $\nabla\cdot(M_1\nabla\Delta U_n)$ is *not* as in a Crank-Nicolson type scheme. The scheme is still consistent with these two added terms since the difference of them goes to zero as the size of time discetization goes to zero. The same observation holds for the other pair of inserted terms involving the constant M_1. The advantage of doing this can be appreciated for example from the consideration of regularity and stability issues.

Even though there is much literature on analysis of finite element methods, there is much less analysis for finite difference schemes solving higher order partial differential equations. The nonlinear schemes such as the one above, although yielding satisfactory theoretical results from the point of view of scheme convergence and stability, are less attractive from the point of view of computational load, in particular for the practitioner who may not have higher order finite element codes at their disposal (or the expertise to quickly adapt them to problems of interest). Also, the nonlinear implicit problem requires the solution of large scale nonlinear algebraic systems at each time discretization step. This problem is perhaps the most computationally prohibitive when solving high order nonlinear partial differential equations in high dimensional physical domains. Since there is demand from the engineering and computational science community for simpler codes, it is therefore important to provide a clear exposition of convergence of simpler linear splitting schemes, in the context of strong (smooth) solutions. Finally we mention that in [4], it is assumed that mobility function f satisfies

$$f\in C(\mathbb{R}),\quad 0\leqslant f_{min}\leqslant f(s)\leqslant f_{max}<+\infty,\quad \forall s\in\mathbb{R}. \tag{1.9}$$

Under the above assumptions and some other technical assumptions, e.g.

$$u_0\in H^3(\Omega),\quad \|u_0\|_\infty<1-\delta,\quad \|U_0\|_\infty\leqslant 1-\delta/2,$$

they prove uniform boundedness of $\|\nabla U_n\|$. As a conventional notation, we denote $\|u(\cdot,t)\|$ and $\|U_n\|$ as the standard L^2 norms for square integralable functions $u(\cdot,t)$ (at t) and $U_n(\cdot)$. Moreover, under further assumption:

$$0 < f_{min} \leqslant f_{max} < +\infty, \quad f \in C^1(\mathbb{R}), \quad \|f'\|_\infty < +\infty, \tag{1.10}$$

and that

$$\|\nabla(u_0 - U_0)\|^2 \leqslant C\Delta t,$$

the half order convergence in time is proven in [4] in the spaces $L^2([0,T], H^1(\Omega))$ and $L^\infty([0,T], (H^1(\Omega))')$. Therefore, for convergence, their assumption on f is essentially the same as ours. For g, instead of a general function ψ which we use here, they use a special function Ψ: which satisfies

$$\Psi'(s) = \frac{\theta}{2} \ln \frac{1+s}{1-s} - \theta_c s.$$

There θ and θ_c are positive constants with $\theta < \theta_c$. This assumption is equivalent to the assumption that

$$\varphi'(s) = \frac{\theta s}{s^2 - 1} - \theta_c.$$

Since both papers by Barrett et. al. and ours deal with only non-degenerate case, we know that $|u|_\infty < 1 - \delta$. Therefore our assumption that g is uniformly bounded and uniformly Lipschitz continuous essentially covers this special case. In the analysis below, we develop a strong convergence theory (for smooth solutions), proving that our scheme converges at the rate of at least $O(\Delta t)$ (see Theorem 3.1), which is higher than the half order rate proved in [4]. The computational examples we provide show further that our scheme is practical and useful.

2. Typical behavior of the scheme and the underlying continuous PDE.

First we review the typical behavior of interest of smooth solutions of the PDE (1.1,1.2). Existence of solutions of the scheme follows from standard elliptic boundary value theory.

2.1. Solutions of the PDE.

Much work has been done in the last twenty years on rigorous (existence, uniqueness, long time behavior) analysis of solutions of fourth order degenerate diffusion equations and on applications. For thin film equations, several review articles for both the theory and applications problems exist including [11, 41, 43]. There are a number of interesting physical problems corresponding to equations of the type considered in this paper. For thin film applications, the problem with $\varphi = 0$ is a degenerate fourth order equation. The case $f(u) = u^3$ corresponds to a thin film of liquid with a no-slip condition on the liquid-solid interface. The case $f(u) = u$ arises in the study of liquid bridges in a Hele-Shaw cell [15, 17]. The case with $\varphi \neq 0$ also arises in a number of 'long-wave' stable and unstable film problems including dewetting films under van der Waals interactions [13, 26], gravity driven layers in a Hele-Shaw cell [27, 28], and thin films spreading under gravity [14].

Another related class of models are the Cahn-Hilliard models with degenerate mobility [20]. In such models f is also typically a polynomial function but can vanish at more than one value of u depending on the application. Recently Glasner has proposed such models as diffuse interface approximations of Hele-Shaw motion [25]. In this case $f(u) = u$ as in the Hele-Shaw example above, however the role of u is no longer the film thickness but instead a phase variable describing the presence or absence of liquid within the cell.

In general we do not have well-posedness results in the case where $f(u)$ vanishes due to the lack of a maximum principle for higher order PDE. Some 'weak maximum principle' pointwise results are known in one space dimension [7, 12] but do not extend to higher dimensions. Nevertheless, for many of the application areas it is reasonable to consider, even in higher dimensions, the existence of strong solutions away from vanishing values of f. In addition to the possibility of u vanishing, in the case of long-wave unstable models, one can consider the possibility of blowup, in which u goes to infinity [10, 8]. Such problems depend on special nonlinear forms of φ.

For the purpose of this paper we focus on cases where there exists a smooth, bounded solution $u(x,t)$ to the continuous PDE such that u avoids values where f vanishes. Since we are interested in bounded solutions, it is natural to consider an arbitrary bound on $f(u)$ for the solution of the PDE. For simplicity in the following analysis, we consider solutions for which $0 < f(u) < 1$, however the upper bound is arbitrary and could trivially be generalized.

It is easy to see that for the exact solution u to (1.4), we have

$$\begin{aligned}\frac{d}{dt}\int_\Omega |\nabla u|^2 dx + 2\int_\Omega f(u)|\nabla\Delta u|^2 dx\\ = 2\int_\Omega g(u)(\nabla u)\cdot\nabla\Delta u\ dx.\end{aligned} \tag{2.1}$$

This formula provides a theoretical basis for a priori H^1 estimates for the equation and there is a natural extension to the schemes considered in this paper.

2.2. **Existence, uniqueness and regularity of U_n.** Due to the simple nature of the scheme, in which the new time level depends only on the solution of a linear fourth order elliptic equation, existence and uniqueness of solutions of the scheme is straightforward. We need to specify boundary conditions for this problem, and that of the underlying PDE. The most common choices for this class of problems, on bounded domains, are the periodic boundary conditions on the torus, and Neumann-type conditions for u and Δu for domains with boundary. The application problems we consider use FFT solvers for the elliptic problem and thus periodic boundary conditions make the most sense for this paper. For any fixed Δt, the equation (1.6) with corresponding boundary conditions forms a standard fourth order elliptic boundary value problem, whose well-posedness is completely solved by the Lax-Milgram lemma.

Moreover, by integrating (1.6) over Ω, we have the following conservation of mass:

$$\int_\Omega U_n dx = \int_\Omega U_0 dx = \int_\Omega u_0 dx = \int_\Omega u_n dx, \quad \forall n \geqslant 1. \tag{2.2}$$

Recall that we assume U_n is the spatial discretization of u at time $t = t_n$, with

$$U_0(x) = u_0(x) = u(x,0), \quad x \in \Omega.$$

3. **Rigorous estimates for the scheme.**

3.1. **Consistency.** The local time truncation error can be computed using standard Taylor series arguments. In the following, we take $M_1 = 1$ for simplicity. The general case can be similarly treated.

Suppose we have a solution u of the continuous PDE (1.4) on the torus T^d, where d is the dimension of the physical domain. Let u_n denote $u(n\Delta t)$. Then the local truncation error is defined over a time step as satisfying

$$\begin{aligned}\frac{u_{n+1}-u_n}{\Delta t}&+\Delta^2 u_{n+1}\\ &-\nabla\cdot[(1-f(u_n))\nabla\Delta u_n+g(u_n)\nabla u_n]=\tau_n,\end{aligned}\tag{3.1}$$

where

$$\tau_n=\tau_{n,1}+\tau_{n,2},$$

with

$$\tau_{n,1}\equiv\frac{u_{n+1}-u_n}{\Delta t}-u_t(n\Delta t)$$

and

$$\tau_{n,2}\equiv\Delta t\Delta^2\frac{u_{n+1}-u_n}{\Delta t}.$$

By Taylor's expansion theorem, we have,

$$\tau_{n,1}=\frac{1}{2\Delta t}\int_{n\Delta t}^{(n+1)\Delta t}u_{tt}(t)\,[(n+1)\Delta t-t]\,dt$$

and

$$\tau_{n,2}=\int_{n\Delta t}^{(n+1)\Delta t}\Delta^2 u_t(t)dt.$$

Therefore,

$$\|\tau_{n,1}\|_{-1}\equiv\|\tau_{n,1}(\cdot,t)\|_{H^{-1}}\leqslant\frac{\Delta t}{2}\max_{n\Delta t\leqslant t\leqslant(n+1)\Delta t}\|u_{tt}(\cdot,t)\|_{-1}$$

and

$$\|\tau_{n,2}\|_{-1}\equiv\|\tau_{n,2}(\cdot,t)\|_{H^{-1}}\leqslant\Delta t\max_{n\Delta t\leqslant t\leqslant(n+1)\Delta t}\|\nabla\Delta u_t(\cdot,t)\|.$$

Assuming that $\|u_{tt}(\cdot,t)\|_{H^{-1}}$ and $\|\nabla\Delta u_t(\cdot,t)\|$ are uniformly bounded with respect to t, we have the following result for consistence of the scheme:

$$\|\tau_n\|_{-1}\equiv\|\tau_n\|_{H^{-1}}=O(\Delta t),\tag{3.2}$$

which is used in our analysis of convergence of the scheme.

3.2. **Boundedness.** In this section, we prove some a priori bounds for numerical solutions that satisfy a basic pointwise bound on the nonlinear diffusion coefficient. For simplicity of analysis we assume $\|f(U_n)\|_\infty\leqslant 1$. Note also that we could replace 1 by a large enough $M_1>0$, satisfying

$$\|f(u(\cdot,\cdot))\|_\infty\leqslant M_1<\infty.$$

In general, such a priori pointwise bounds are difficult to prove for thin film equations in higher space dimensions. In one dimension the result follows directly from an *a priori* H1 bound and Sobolev embedding. See [7, 9, 8]. However H1 control does not imply a pointwise bound in dimensions two and higher.

Nevertheless, for practical reasons, as shown in our computational section, it is reasonable to consider numerical solutions that happen to satisfy

$$\|f(U_n)\|_\infty\leqslant M_1<\infty,\tag{3.3}$$

and in fact this can be used as an a posteriori constraint on the timestep.

We have the following estimate. Taking the inner product with $-\Delta U_{n+1}$, and letting $\|\cdot\|$ denote the L^2 norm, we have

$$\begin{aligned}
&\frac{1}{2\Delta t}(\|\nabla U_{n+1}\|^2 - \|\nabla U_n\|^2)\\
&\quad + \frac{1}{2\Delta t}\|\nabla(U_{n+1} - U_n)\|^2 + \|\nabla\Delta U_{n+1}\|^2\\
=&\frac{1}{\Delta t}(\nabla(U_{n+1} - U_n), \nabla U_{n+1}) - (\Delta^2 U_{n+1}, \Delta U_{n+1})\\
=&((1 - f(U_n))\nabla\Delta U_n, \nabla\Delta U_{n+1}) + (g(U_n)\nabla U_n, \nabla\Delta U_{n+1})\\
\leqslant& \int_\Omega (1 - f(U_n))\frac{|\nabla\Delta U_n|^2 + |\nabla\Delta U_{n+1}|^2}{2}dx\\
&\quad + \int_\Omega g(U_n)\nabla U_n \cdot \nabla\Delta U_{n+1}dx,
\end{aligned}$$

where in the last step, we have used the assumption that $\|f(U_n)\|_\infty \leqslant 1$. Thus

$$\begin{aligned}
&\frac{1}{\Delta t}\left(\|\nabla U_{n+1}\|^2 - \|\nabla U_n\|^2\right) + \|\nabla\Delta U_{n+1}\|^2 - \|\nabla\Delta U_n\|^2\\
&\quad + \int_\Omega f(U_n)(|\nabla\Delta U_n|^2 + |\nabla\Delta U_{n+1}|^2)dx\\
&\leqslant 2\int_\Omega g(U_n)\nabla U_n \cdot \nabla\Delta U_{n+1}dx.
\end{aligned} \tag{3.4}$$

Remark 1: Notice that (3.4) is an interesting approximation of (2.1). If $g = 0$, the above result implies an estimate of the form

$$\|\nabla U_{n+1}\|^2 + \Delta t\|\nabla\Delta U_{n+1}\|^2 \leqslant \|\nabla U_n\|^2 + \Delta t\|\nabla\Delta U_n\|^2$$

over the timestep, providing uniformly boundedness of U_n in H^1 provided that $\|\Delta\nabla u_0\|$ is bounded. The other assumption needed for this estimate is the uniform pointwise bound $f(U_n) \leqslant 1$ (or less than a specified constant) which can be implemented as an a posteriori restriction on the timestep. We present computational examples of this implementation later in the paper.

In general, one has $f(U_n) \leqslant M$. However for simplicity of notation we perform the analysis for the problem scaled so that $f(U_n) \leqslant 1$.

□

For the general case, we have

$$\begin{aligned}
&\frac{1}{\Delta t}(\|\nabla U_{n+1}\|^2 - \|\nabla U_n\|^2) + \|\nabla\Delta U_{n+1}\|^2\\
&\quad - \|\nabla\Delta U_n\|^2 + \int_\Omega f(U_n)|\nabla\Delta U_n|^2dx\\
&\leqslant \int_\Omega \frac{g^2(U_n)}{f(U_n)}|\nabla U_n|^2dx.
\end{aligned}$$

Assume that

$$C_0 := \left\|\frac{g^2}{f}\right\|_\infty < +\infty. \tag{3.5}$$

Then,

$$\begin{aligned}
\|\nabla U_{n+1}\|^2 +& \Delta t\|\nabla\Delta U_{n+1}\|^2\\
&\leqslant (1 + C_0\Delta t)(\|\nabla U_n\|^2 + \Delta t\|\nabla\Delta U_n\|^2).
\end{aligned}$$

By induction, we have, for $n\Delta t \leqslant T$,

$$\begin{aligned}\|\nabla U_n\|^2 + &\Delta t\|\nabla\Delta U_n\|^2 \\ &\leqslant (1 + C_0\Delta t)^n(\|\nabla U_0\|^2 + \Delta t|\nabla\Delta U_0\|^2) \\ &\leqslant e^{C_0T}(\|\nabla U_0\|^2 + \Delta t|\nabla\Delta U_0\|^2),\end{aligned} \tag{3.6}$$

which gives boundedness of the solution sequence on $[0,T]$ for any $T > 0$.

Remark 2: Assuming (3.5), we have,

$$\begin{aligned}\frac{1}{2}\frac{d}{dt}\int_\Omega |\nabla u|^2 dx =& -\int_\Omega f(u)|\nabla\Delta u|^2 dx + \int_\Omega g(u)\nabla u\cdot\nabla\Delta u dx \\ =& -\int_\Omega f(u)\left|\nabla\Delta u + \frac{1}{2}\frac{g(u)}{f(u)}\nabla u\right|^2 dx \\ &+ \frac{1}{4}\int_\Omega \frac{g^2(u)}{f(u)}|\nabla u|^2 dx \\ \leqslant& \frac{1}{4}\left\|\frac{g^2(u)}{f(u)}\right\|_\infty \int_\Omega |\nabla u|^2 \\ =& \frac{C_0}{4}\int_\Omega |\nabla u|^2 dx.\end{aligned} \tag{3.7}$$

Therefore, by Grönwall inequality, we have

$$\|\nabla u(t)\| \leqslant \|\nabla u_0\| e^{\frac{C_0}{2}t}.$$

Notice that (3.6) gives an estimate of U_n which reflects nicely that of u as shown above.

□

3.3. **Convergence.** In this section we prove convergence of the scheme in H^1 provided that we have a smooth solution of the PDE *and* that a solution of the scheme exists satisfying the a posteriori bound

$$0 < \epsilon_0 < f(U_n) < 1. \tag{3.8}$$

Again, the constant 1 is chosen for convenience; however the argument below extends to any suitable upper bound. In practice one can often achieve the bound (3.8) by a suitable a posteriori time step control. This is demonstrated in a number of examples in section 4.

Let $e_n = u_n - U_n$. By (1.6) and (3.1), we have

$$\begin{aligned}\frac{1}{\Delta t}(e_{n+1} - e_n) + \Delta^2 e_{n+1} =& \nabla\cdot((1 - f(u_n))\nabla\Delta u_n) \\ &- \nabla\cdot((1 - f(U_n))\nabla\Delta U_n) \\ &+ \nabla\cdot[g(u_n)\nabla u_n - g(U_n)\nabla U_n] + \tau_n.\end{aligned} \tag{3.9}$$

Taking inner product with $-\Delta e_{n+1}$, we have

$$\begin{aligned}\frac{1}{\Delta t}(\nabla e_{n+1} - &\nabla e_n, \nabla e_{n+1}) + \|\nabla\Delta e_{n+1}\|^2 \\ =& ((1 - f(u_n))\nabla\Delta u_n - (1 - f(U_n))\nabla\Delta U_n, \nabla\Delta e_{n+1}) \\ &+ (g(u_n)\nabla u_n - g(U_n)\nabla U_n, \nabla\Delta e_{n+1}) \\ &+ (\nabla\Delta^{-1}\tau_n, \nabla\Delta e_{n+1}).\end{aligned}$$

Therefore,

$$\begin{aligned}\frac{\|\nabla e_{n+1}\|^2-\|\nabla e_n\|^2}{2\Delta t}&+\|\nabla\Delta e_{n+1}\|^2\\ &\leqslant((1-f(U_n))\nabla\Delta e_n,\nabla\Delta e_{n+1})\\ &\quad-((f(u_n)-f(U_n))\nabla\Delta u_n,\nabla\Delta e_{n+1})\\ &\quad-(g(U_n)\nabla e_n,\nabla\Delta e_{n+1})\\ &\quad+((g(u_n)-g(U_n))\nabla u_n,\nabla\Delta e_{n+1})\\ &\quad+(\nabla\Delta^{-1}\tau_n,\nabla\Delta e_{n+1}).\end{aligned}$$

Assuming that $f(U_n)\leqslant 1$, then we have as before,

$$\begin{aligned}\frac{\|\nabla e_{n+1}\|^2-\|\nabla e_n\|^2}{\Delta t}&+\|\nabla\Delta e_{n+1}\|^2-\|\nabla\Delta e_n\|^2\\ &+\int_\Omega f(U_n)\left(|\nabla\Delta e_n|^2+|\nabla\Delta e_{n+1}|^2\right)dx\\ &\leqslant-2((f(u_n)-f(U_n))\nabla\Delta u_n,\nabla\Delta e_{n+1})\\ &\quad-2(g(U_n)\nabla e_n,\nabla\Delta e_{n+1})\\ &\quad+2((g(u_n)-g(U_n))\nabla u_n,\nabla\Delta e_{n+1})\\ &\quad+2(\nabla\Delta^{-1}\tau_n,\nabla\Delta e_{n+1})\\ &\equiv I_1+I_2+I_3+I_4.\end{aligned}$$

Using Cauchy-Schwartz inequality, we have

$$\begin{aligned}I_1\leqslant C&\int_\Omega\frac{|\nabla\Delta u_n|^2}{f(U_n)}|f(u_n)-f(U_n)|^2dx\\ &+\frac{1}{8}\int_\Omega f(U_n)|\nabla\Delta e_{n+1}|^2dx,\end{aligned}$$

$$\begin{aligned}I_2\leqslant C&\int_\Omega\frac{g^2(U_n)}{f(U_n)}|\nabla e_n|^2dx\\ &+\frac{1}{8}\int_\Omega f(U_n)|\nabla\Delta e_{n+1}|^2dx,\end{aligned}$$

$$\begin{aligned}I_3\leqslant C&\int_\Omega\frac{|\nabla u_n|^2}{f(U_n)}|g(u_n)-g(U_n)|^2dx\\ &+\frac{1}{8}\int_\Omega f(U_n)|\nabla\Delta e_{n+1}|^2dx,\end{aligned}$$

and

$$\begin{aligned}I_4\leqslant C&\int_\Omega\frac{1}{f(U_n)}|\nabla\Delta^{-1}\tau_n|^2dx\\ &+\frac{1}{8}\int_\Omega f(U_n)|\nabla\Delta e_{n+1}|^2dx.\end{aligned}$$

Assume that f and g are Lipschitz continuous, $|\nabla\Delta u_n|$, $|\nabla u_n|$, $|g(U_n)|$ are uniformly bounded from above and that $f(U_n)$ is uniformly bounded from below.

Then, we have

$$\begin{aligned}\frac{\|\nabla e_{n+1}\|^2 - \|\nabla e_n\|^2}{\Delta t} &+ \|\nabla\Delta e_{n+1}\|^2 - \|\nabla\Delta e_n\|^2 \\ &+ \int_\Omega f(U_n)\left(|\nabla\Delta e_n|^2 + \frac{|\nabla\Delta e_{n+1}|^2}{4}\right)dx \\ &\leqslant C\|\nabla e_n\|^2 + C\|\tau_n\|_{-1}^2,\end{aligned}$$

where we have used the Poincaré inequality, noticing that e_n is mean-zero.

So,

$$\begin{aligned}\|\nabla e_{n+1}\|^2 &+ \|\nabla\Delta e_{n+1}\|^2\Delta t \\ &\leqslant (1+C\Delta t)\|\nabla e_n\|^2 + \|\nabla\Delta e_n\|^2\Delta t + C\|\tau_n\|_{-1}^2\Delta t \\ &\leqslant (1+C\Delta t)\left[\|\nabla e_n\|^2 + \|\nabla\Delta e_n\|^2\Delta t\right] + C\|\tau_n\|_{-1}^2\Delta t.\end{aligned}$$

By induction on n and assuming $e^0 = 0$, we have

$$\|\nabla e_n\| + \|\nabla\Delta e_n\|\sqrt{\Delta t} \leqslant C\sqrt{n\Delta t}e^{\frac{n\Delta t}{2}}\max_{k\leqslant n}\|\tau_k\|_{-1}. \tag{3.10}$$

Recall that consistency of the scheme yields

$$\max_n \|\tau_n\|_{-1} = O(\Delta t). \tag{3.11}$$

Therefore, we have

$$\|\nabla e_n\| + \|\nabla\Delta e_n\|\sqrt{\Delta t} \leqslant C\sqrt{T}e^{\frac{T}{2}}\Delta t. \tag{3.12}$$

Remark 3: From the above analysis, we see that we have first order convergence in H^1 norm and a half order convergence in H^3 norm, provided that f, g are Lipschitz continuous, $|\nabla\Delta u_n|$, $|\nabla u_n|$, $|g(U_n)|$ are uniformly bounded from the above and $|f(U_n)|$ satisfies (3.8). Using the method of induction, we can prove the same convergence result when dropping the above assumptions on the discrete solution U_n to the numerical scheme, with a few more assumptions on the solution u to the original partial differential equation.

□

Theorem 3.1. *Suppose that for $t \in [0,T]$, $\nabla u, \nabla\Delta u$ are uniformly bounded, f, g are Lipschitz continuous with Lipschitz constants L_f and L_g respectively, and there exist constants c_1, c_2, such that*

$$0 < c_1 \leqslant |u(x,t)| \leqslant c_2, \quad \forall (x,t) \in \Omega \times [0,T]$$

and

$$0 < \delta \leqslant f(u) \leqslant M_f < 1, \quad |g(u)| \leqslant M_g < +\infty.$$

Then, there exists constants $C_1, C_2 > 0$ and $\Delta t_0 > 0$, such that for all Δt with $0 < \Delta t < \Delta t_0$ and $n\Delta t \leqslant T$, we have

$$\|\nabla e_n\| + \|\nabla\Delta e_n\|\sqrt{\Delta t} \leqslant C_0\sqrt{T}e^{\frac{C_1 T}{2}}\sup_{n\Delta t\leqslant T}\|\tau_n\|_{-1}. \tag{3.13}$$

Moreover, we have $0 < c_1 - \epsilon \leqslant |U_n| \leqslant c_2 + \epsilon$ and thus

$$0 < \delta - \varepsilon \leqslant f(U_n) \leqslant M_f + \varepsilon < 1. \tag{3.14}$$

and that U_n is uniformly bounded for $n\Delta t \leqslant T$ in H^m for $0 \leqslant m \leqslant 3$.

Proof. We use the method of induction.

First of all, we have $e_0 = 0$. Therefore the error estimate (3.13) is automatically satisfied for $n = 0$. Moreover, we have

$$0 < \delta \leqslant f(U_n) = f(u_n) \leqslant M_f < 1.$$

Then, we have

$$\begin{aligned}\frac{1}{2\Delta t}\|\nabla e_1\|^2 + \frac{1}{2}\|\nabla\Delta e_1\|^2 + \frac{1}{2}\int_\Omega f(u_0)|\nabla\Delta e_1|^2 dx \\ \leqslant -(\tau_0, \Delta e_1) \leqslant 4\|\tau_0\|_{-1}^2 + \frac{1}{4}\|\nabla\Delta e_1\|^2.\end{aligned}$$

Therefore,

$$\|\nabla e_1\|^2 + \|\nabla\Delta e_1\|^2\Delta t \leqslant C\Delta t\|\tau_0\|_{-1}^2, \tag{3.15}$$

where C is a constant independent of Δt. Thus, (3.13) is satisfied for $n = 1$. For Δt small enough, which will be specified later, we have that for $n \leqslant 1$,

$$0 < c_1 - \epsilon < |U_n| < c_2 + \epsilon,$$

and thus

$$0 < \delta - \varepsilon \leqslant f(U_n) \leqslant M_f + \varepsilon < 1, \tag{3.16}$$

$$|g(U_n)| \leqslant M_g + \varepsilon. \tag{3.17}$$

Hence,

$$\begin{aligned}\frac{\|\nabla e_2\|^2 - \|\nabla e_1\|^2}{\Delta t} &+ \left(\|\nabla\Delta e_2\|^2 - \|\nabla\Delta e_1\|^2\right) \\ &+ \int_\Omega f(U_1)(|\nabla\Delta e_1|^2 + \|\nabla\Delta e_2\|)dx \\ &\leqslant -2((f(u_1) - f(U_1))\nabla\Delta u_1, \nabla\Delta e_2) \\ &\quad - 2(g(U_1)\nabla e_1, \nabla\Delta e_2) \\ &\quad + 2((g(u_1) - (U_1))\nabla u_1, \nabla\Delta e_2) \\ &\quad - 2(\tau_1, \Delta e_2) \\ &\equiv I_1 + I_2 + I_3 + I_4.\end{aligned}$$

Therefore,

$$\begin{aligned}\frac{\|\nabla e_2\|^2 - \|\nabla e_1\|^2}{\Delta t} &+ \|\nabla\Delta e_2\|^2 - \|\nabla\Delta e_1\|^2 \\ &+ (\delta - \varepsilon)(\|\nabla\Delta e_1\|^2 + \|\nabla\Delta e_2\|^2) \\ &\leqslant I_1 + I_2 + I_3 + I_4.\end{aligned}$$

We estimate I_i's ($i = 1, \dots, 4$) in the following one by one.

$$\begin{aligned}I_1 &\leqslant 2L_f\|\nabla\Delta u_1\|_\infty\|e_1\|\|\nabla\Delta e_2\| \\ &\leqslant \frac{8L_f^2\|\nabla\Delta u_1\|_\infty^2}{\delta - \varepsilon}\|e_1\|^2 + \frac{\delta - \varepsilon}{8}\|\nabla\Delta e_2\|^2,\end{aligned}$$

$$\begin{aligned}I_2 &\leqslant 2(M_g + \varepsilon)\|\nabla e_1\|\|\nabla\Delta e_2\| \\ &\leqslant \frac{8(M_g + \varepsilon)^2}{\delta - \varepsilon}\|\nabla e_1\|^2 + \frac{\delta - \varepsilon}{8}\|\nabla\Delta e_2\|^2,\end{aligned}$$

$$
\begin{aligned}
I_3 &\leqslant 2L_g\|\nabla u_1\|_\infty\|e_1\|\|\nabla\Delta e_2\| \\
&\leqslant \frac{8L_g^2\|\nabla u_1\|_\infty^2}{\delta-\varepsilon}\|e_1\|^2+\frac{\delta-\varepsilon}{8}\|\nabla\Delta e_2\|^2,
\end{aligned}
$$

and

$$
\begin{aligned}
I_4 &= 2(\nabla\Delta^{-1}\tau_1,\nabla\Delta e_2) \\
&\leqslant \frac{8}{\delta-\varepsilon}\|\tau_1\|_{-1}^2+\frac{\delta-\varepsilon}{8}\|\nabla\Delta e_2\|^2.
\end{aligned}
$$

Hence,

$$
\begin{aligned}
(\|\nabla e_2\|^2+&\Delta t\|\nabla\Delta e_2\|^2)-(\|\nabla e_1\|^2+\Delta t\|\nabla\Delta e_1\|^2) \\
&+(\delta-\varepsilon)\|\nabla\Delta e_1\|^2\Delta t+\frac{\delta-\varepsilon}{2}\|\nabla\Delta e_2\|^2\Delta t \\
&\leqslant C_2\|\nabla e_1\|^2\Delta t+C_1\Delta t\|\tau_1\|_{-1}^2,
\end{aligned}
$$

where we have used the Poincaré inequality with the Poincaré constant denoted by c_p, the positive constant C_1 defined as

$$
C_1=\frac{8}{\delta-\varepsilon}, \tag{3.18}
$$

and the positive constant C_2 satisfying

$$
\begin{aligned}
\frac{C_2(\delta-\varepsilon)}{8} =&L_f^2\sup_{n\Delta t\leqslant T}\|\nabla\Delta u_n\|_\infty^2c_p^2+(M_g+\varepsilon)^2 \\
&+L_g^2\sup_{n\Delta t\leqslant T}\|\nabla u_n\|_\infty^2c_p^2.
\end{aligned} \tag{3.19}
$$

Then,

$$
\begin{aligned}
\|\nabla e_2\|^2+&\Delta t\|\nabla\Delta e_2\|^2 \\
&\leqslant(1+C_2\Delta t)\left(\|\nabla e_1\|^2+\Delta t\|\nabla\Delta e_1\|^2\right) \\
&\quad+C_1\Delta t\sup_{k\geqslant 1}\|\tau_k\|_{-1}^2.
\end{aligned}
$$

Thus, by one iteration or applying the discrete Grönwall inequality, we have

$$
\begin{aligned}
\|\nabla e_2\|^2+&\Delta t\|\nabla\Delta e_2\|^2+\frac{\Delta t(\delta-\varepsilon)}{2}\|\nabla\Delta e_2\|^2 \\
&\leqslant C_1Te^{2C_2\Delta t}\sup_{k\geqslant 1}\|\tau_k\|_{-1}^2.
\end{aligned}
$$

Therefore, (3.13) is satisfied for $n=2$.

In general, if (3.13) is satisfied for $n=k$ and Δt is small enough, say no greater than a constant Δt_0 which can be decided by the value of C_1 and C_2 as given by (3.18) and (3.19) and by (3.13), then (3.16) and (3.17) are satisfied for $n\leqslant k$. Notice that, due to (3.13), for (3.16) and (3.17) to be valid, the restriction on Δt_0 may depend on T, but is independent of k for $k\Delta t\leqslant T$. Therefore similar argument in obtaining the error estimate for $n=2$ is now valid for $n=k+1$ and we get exactly (3.13) with $n=k+1$, with the *same* coefficients C_1 and C_2 as given by (3.18) and (3.19). So by induction, (3.13) is valid for all n such that $n\Delta t\leqslant T$, provided that Δt is small enough.

Moreover, recalling that $\|\tau\|_{-1}$ is $O(\Delta t)$, we have the upper bounds for $|U_n|$, $|\nabla U_n|$ and $|\nabla\Delta U_n|$ which are *uniform* for all $n\leqslant T/\Delta t$ and thus the bounds on $f(U_n)$ and $g(U_n)$ as well. □

4. **Numerical simulations and discussion.** We investigate the numerical properties of the biharmonic modified forward time-stepping for different variations of the fourth order nonlinear equations (1.1)-(1.2). For convenience, the finite differencing scheme is repeated here,

$$\frac{u^{n+1}-u^n}{\Delta t}+M\Delta^2 u^{n+1}=\nabla\cdot\left(\left(M-f\left(u^n\right)\right)\nabla\Delta u^n\right)+\nabla\cdot\left(f\left(u^n\right)\nabla\varphi'\left(u^n\right)\right). \quad (4.1)$$

We choose the scalar $M=\alpha\max\left(f\left(u^n\right)\right)$ and vary the value of α to investigate the effect of M on the numerical stability. The equation is discretized on a uniform cartesian mesh where $u^n_{i,j}=u(x_i,y_j,t^n)$, $x_i=i\Delta x$, and $y_j=j\Delta x$. We formulate the spatial finite difference in conservative form,

$$\begin{aligned}
\mathbf{Q} &= (p,q)^T=\left(\left(M-f\left(u^n\right)\right)\nabla\Delta u^n+f\left(u^n\right)\nabla\varphi'\left(u_n\right)\right), && (4.2)\\
\nabla\cdot\mathbf{Q} &= \delta_x p+\delta_y q, && (4.3)\\
\delta_x p &= \frac{\left(p_{i+1/2,j}-p_{i-1/2,j}\right)}{\Delta x},\delta_y q=\frac{\left(q_{i,j+1/2}-q_{i,j-1/2}\right)}{\Delta x}.
\end{aligned}$$

The mobility terms at the midpoints of the mesh are approximated by trapezoidal averages

$$f\left(u_{i+1/2,j}\right)=f\left(\frac{1}{2}\left[u_{i,j}+u_{i+1,j}\right]\right), \quad (4.4)$$

and similarly for $f(u_{i,j+1/2})$. The spatial operators on u can then be formulated using second-order central difference on the existing grid points. We impose Neumann boundary conditions on the domain boundary. Note that this is equivalent to periodic boundary conditions with symmetry imposed (and thus connects directly to the theory from the previous section). The constant linear implicit operator can be inverted efficiently using fast Fourier transform. A step doubling scheme is used to adjust the simulation timesteps and a local extrapolation [44] removes the $O(\Delta t)$ truncation error.

We first verify the convergence of the numerical scheme in the case of a well-known 2D self-similar solution of a simple fourth order lubrication equation. We will then illustrate interesting dynamics that arises in coarsening and in microfluidics through the coupling of the fourth order operator with various energy terms.

4.1. **Lubrication equation.** Defining $\varphi'=0$ and $f\left(u\right)=u$ reduces equations (1.1)-(1.2) to a nonlinear fourth order diffusion equation,

$$u_t+\nabla\cdot\left(u\nabla\Delta u\right)=0. \quad (4.5)$$

The equation dissipates a free energy of the form

$$\frac{d\mathcal{E}}{dt}=-\int_\Omega|\nabla u|^2dx\le 0. \quad (4.6)$$

There exists a compactly-supported, d-dimensional, radially-symmetric self-similar solution [22]

$$\begin{aligned}
u\left(\eta,t\right) &= \begin{cases}\frac{1}{8(d+2)\tau^d}\left(L^2-\eta^2\right)^2 & ,\quad 0\le\eta\le L\\ 0 & ,\quad \eta>L,\end{cases} && (4.7)\\
\tau &= \left[\left(d+4\right)\left(t+t_0\right)\right]^{1/(d+4)}, && (4.8)
\end{aligned}$$

where $\eta=r/t$.

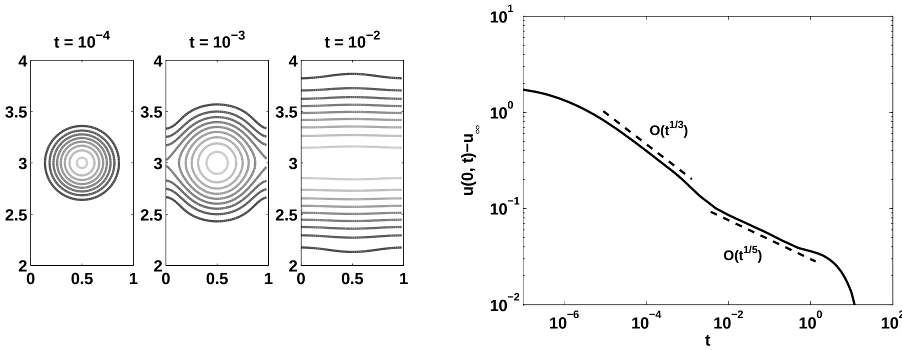

(A) (B)

FIGURE 1. (a) Contours of the simulated solution of the nonlinear lubrication equation (4.5) starting from initial condition (4.10) at various simulation time. (b)Evolution of the maximum of the thin film, $u(r=0,t)$.

In addition to the stability constraint imposed by the fourth order operator, the degenerate mobility requires a specialized numerical scheme to preserve positivity of the solution. We regularize (4.5) by replacing the degenerate mobility term with

$$f_\xi = \frac{u^5}{(\xi u + u^4)}. \tag{4.9}$$

$\xi = 10^{-10}$ so $f_\xi \sim u$ for $u \gg \xi$. Starting from a Gaussian positive initial data

$$u\,(r,0) = \varepsilon + \frac{\sigma}{40} e^{-\sigma r^2}, \tag{4.10}$$

where $r^2 = x^2 + y^2$, we expect a positive solution of the smooth problem. We solve (4.5) on a 50×500 mesh with $\Delta x = 0.02$, starting from initial condition (4.10) with $\sigma = 80$. The parameter $\varepsilon = 0.01$ specifies a small thickness of the precursor film. The prefactor for the biharmonic modification, $M = \alpha \max\left(f\left(u^n\right)\right)$, is implemented with $\alpha = 0.3$. Figure 1b shows the maximum height of the thin film decreases initially with the $u\,(r=0,t) \sim t^{1/3}$ scaling law of the similarity solution as the film spreads isotropically. Due to the high aspect ratio of the computational domain, the diffusion across the shorter dimension saturates by time $t \sim \mathrm{O}\left(10^{-3}\right)$. The ensuing evolution afterward follows that of a one dimensional problem where $u\,(r=0,t) \sim t^{-1/5}$.

In addition to the dissipation of the free energy, the estimate in Sec. 3.2 implies

$$\|\nabla u^{n+1}\|_{L^2}^2 + \Delta t M \|\nabla \Delta u^{n+1}\|_{L^2}^2 \le \|\nabla u^n\|_{L^2}^2 + \Delta t M \|\nabla \Delta u^n\|_{L^2}^2. \tag{4.11}$$

As shown in figure 2, the biharmonically modified algorithm also dissipates the quantity $F_n = \|\nabla u^n\|_{L^2}^2 + \Delta t M \|\nabla \Delta u^n\|_{L^2}^2$. This provides a convenient way for validating the algorithm.

An adaptive time stepping schemes is implemented to increase the future time step if the numerical solution of the current time step satisfies the dissipation of energy, (4.6). Keeping tract of the maximum of the time step allows us to determine the maximum gradient stable timestep, Δt_g at various stages of the evolution. The

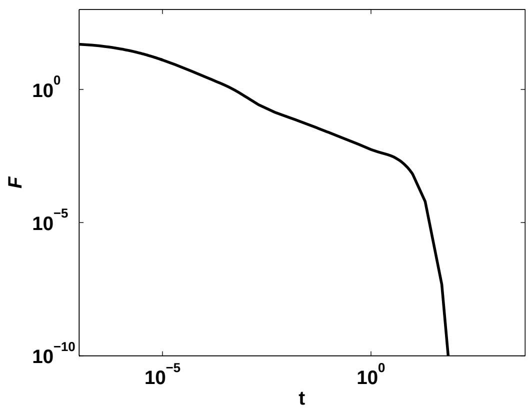

FIGURE 2. Monotonic decrease of the energy estimate, F. Simulation computed using $\alpha = 3.0$.

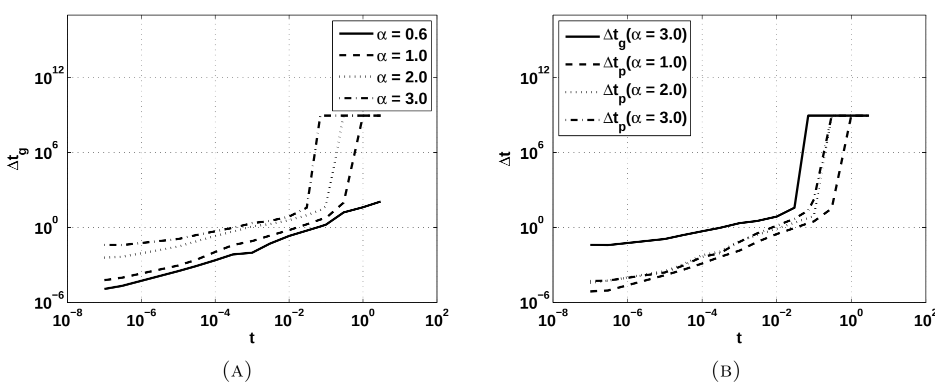

FIGURE 3. (a)Maximum gradient stable timestep, Δt_g. (b)Maximum positivity preserving timesteps, Δt_p, computed with various values of α compared with Δt_g computed with $\alpha = 3.0$.

maximum positivity preserving timestep, Δt_p, are determined by an similar adaptive time stepping scheme that increases the time step with respect to the positivity of the numerical solution. As shown in figure 3a, Δt_g increases with the value of α. As the solution smoothes sufficiently beyond $t \sim 10^{-2}$, unconditional gradient stability is achieved for $\alpha \geq 1.0$. However, figure 3b shows the positivity preserving criterion imposes a stiffer stability requirement that is relatively independent of the value of α.

The accuracy requirement imposes another limiting factor in the simulation. In the Appendix, we derive a modified equation for the the biharmonic modified scheme

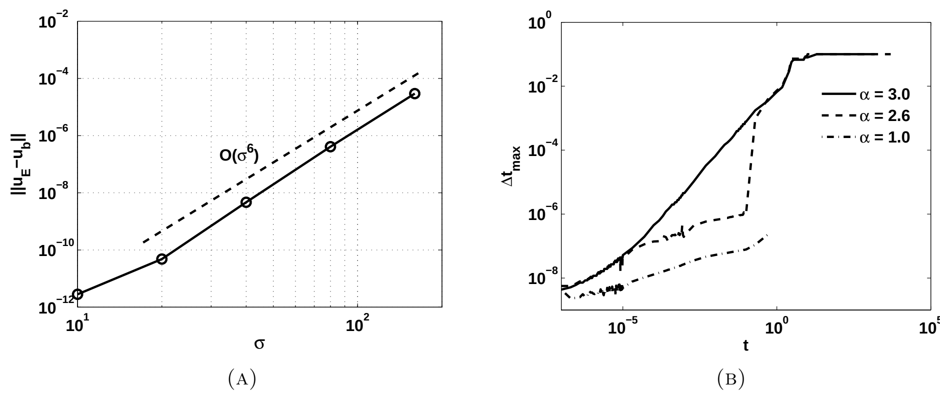

FIGURE 4. (a)Scaling of the truncation error associated with the biharmonic modification. (b)Maximum timestep adopted by the step doubling scheme.

in one dimension,

$$\begin{aligned} u_t + (\mathcal{F}(u))_x &= -\Delta t \left[\left(\frac{\partial \mathcal{F}}{\partial u} (\mathcal{F}(u))_x \right)_x - M(\mathcal{F}(u))_{xxxxx} \right] + O\left(\Delta x^2 + \Delta t^2\right), \\ \mathcal{F}(u) &= u u_{xxx}. \end{aligned} \tag{4.12}$$

The first $O(\Delta t)$ term is the truncation error of the forward Euler timestepping. The biharmonic modification contributes a non-local term in the truncation error. Starting from one dimensional $(r = x)$ Gaussian initial conditions with various σ, we compute the differences of the 1D numerical solutions obtained by the the biharmonic modified timestepping, $u_b(x)$, and by the forward Euler timestepping, $u_E(x)$, after a very small timestep, $\Delta t = 10^{-10}$. Assuming the numerical solutions approximate the Gaussian initial condition, with the characteristic dimensions $x \sim \sigma^{-1/2}$, the truncation error of the biharmonic modification then scales as $||u_E - u_b|| \sim (\mathcal{F}(u))_{xxxxx} \sim \sigma^6$, as confirmed in figure 4a. Therefore, the choice of α must balance the requirements of numerical efficiency and accuracy. It will be interesting to develop a rigorous theory that systematically determines the optimal value of α.

For control of truncation error, we consider a step doubling scheme, which estimates the truncation error by computing $\Delta u = u^{(1)} - u^{(2)}$, where $u^{(1)}$ is the solution after one step of size Δt, and $u^{(2)}$ is the solution after two steps of size $\Delta t/2$. The step doubling adopts the timestep to satisfy a specific accuracy requirement:

$$\frac{2|\Delta u|}{u^{(1)} + u^{(2)}} < 10^{-5}. \tag{4.13}$$

Figure 4b shows the maximum of the adaptive timesteps at various stages of the simulation shown in figure 1. The accuracy criterion places a more stringent constraint on the simulation than the gradient stability. The shape dependent truncation error of the biharmonic modification decreases with the gradient of the numerical solution, allowing the simulation to progressively increase the step size. In contrast, forward Euler timestepping is restricted by a constant stability constraint, $\Delta t \sim O(\Delta x^4) \cong 10^{-8}$. Increasing the value of α beyond 1 allows the simulation to take larger timesteps. Setting $\alpha = 1$ constrains $\Delta t \leq 10^{-6}$, making simulation to steady state impractical.

4.2. **Degenerate Cahn-Hilliard equation.** After studying the numerical behaviors of the biharmonic modified scheme, we now illustrate its application on the Cahn-Hilliard equation with degenerate mobility

$$\epsilon u_t = \nabla \cdot (u \nabla (w)), \tag{4.14}$$

$$w = \left(-\epsilon^2 \triangle u + \varphi'(u)\right). \tag{4.15}$$

A double well function, $\varphi(u) = (u-\varepsilon)^2(u-1)^2$, represents the bulk free energy of the material. The parameter ϵ determines the diffuse interface thickness by balancing the surface energy term, $|\nabla u|^2$, with the bulk free energy, φ. Within this length scale, the phase variable varies smoothly from $u = 1$ to $u = \varepsilon$. The material interface is considered as one of the contours of the phase field variable. In the asymptotic limit of $\epsilon \to 0$, equations (4.14-4.15) approach the sharp interface Hele-Shaw equations.

Equation (4.14-4.15) was first introduced as a model for spinodal decomposition in binary alloys. Such coarsening phenomenon occurs in other systems such as multiphasic fluid and biological swarming. The growth of an ordered domain typically obeys the power law $L \sim t^n$ where L is the length scale of the domain. The detailed understanding of the scaling law, such as the value of n, is difficult to obtain analytically. Therefore, efficient simulation of the phase field model is important to the characterization of the coarsening process.

We initialize the phase field variable randomly on a mesh of size 512×512 with $\Delta x = 0.03$. The diffuse interface thickness imposes a requirement on the grid resolution in order to resolve the transition layer, $\Delta x \leq C\epsilon$. The parameter $\epsilon = 0.0427$ controls the diffuse interface to be $\sim 7\Delta x$. Preconditioning techniques may be implemented to the stability [23]. However, no preconditioning is used in this study.

Figure 10 shows the simulation of the coarsening process. The initial condition quickly coarsens into many smaller domains of irregular shapes with large curvatures, which drive the subsequent interfacial motion to relax the shapes toward circles. The coarsening is due to the interface motion in the diffuse interface approximation, which maintains the phase field variable at a small nonzero value to represent the materials in the dark region. Studies of dewetting thin films have shown coarsening occur in a slow time scale by leakage of material between two disconnected domains [24]. We can not expect this phenomenon to happen in the sharp interface limit. In our coarsening simulation, we did not observe coarsening by this mechanism.

As shown in the introduction, (4.14-4.15) has an energy functional of the form

$$\mathcal{E}(u) = \int_\Omega \frac{\epsilon^2}{2}|\nabla u|^2 + \varphi(u)\, dx, \tag{4.16}$$

which must decrease monotonically for all solutions. Figure 5 shows that biharmonic modified timestepping reproduces such property of the problem.

4.3. **Electrowetting on Dialetctric (EWOD).** A recent study [39] by two of the authors and collaborators considers a phase field model for drop motion, in a Hele-Shaw geometry, due to electrowetting. The model consists of a spatially

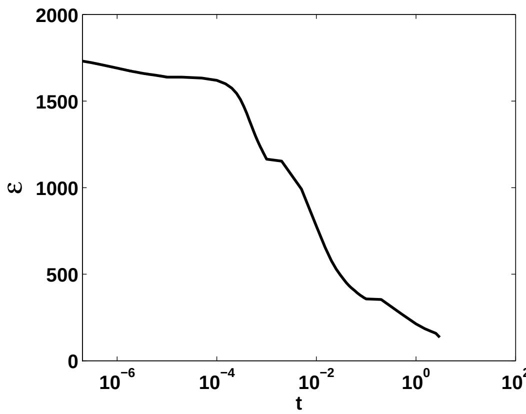

FIGURE 5. Monotonic decrease of the energy functional during the coarsening process.

dependent energy, evolved by a degenerate Cahn-Hilliard equation,

$$\epsilon u_t = \nabla \cdot (u \nabla (w)), \tag{4.17}$$

$$w = \left(-\epsilon^2 \triangle u + \varphi'(u)\right) - \epsilon \beta(x), \tag{4.18}$$

where $\beta(x) = \lambda \chi(x)$ defines a local energy with a characteristic function, $\chi(x)$. An electric field applied across the liquid-solid interface of a fluid drop produces an electrowetting effect that was first characterized by Lippmann [38].

$$\gamma_{sl}(V) = \gamma_{sl}(0) - \frac{1}{2} c V^2, \tag{4.19}$$

where γ_{sl} is the solid-liquid interfacial energy, c is the capacitance per area of the electric double layer, and V is the voltage across the electric double layer. Since $\gamma_{sl}(0)$ is a constant that does not affect the dynamics, we will assume it to be zero. We define $\lambda = cV^2/2\alpha\gamma_{sl}$, where $\alpha = h/R$ is the aspect ratio of the drop, to account for the local electrowetting effect. Zero flux of energy and mass are imposed at the domain boundary

$$\nabla u \cdot \hat{\boldsymbol{n}} = 0, \tag{4.20}$$

$$u \nabla (w) \cdot \hat{\boldsymbol{n}} = 0. \tag{4.21}$$

We solve the problem on a 180×120 mesh with $\Delta x = 1/30$. For this problem, we found $M = 1.0$ is adequate to provide good performance of the scheme.

The electrowetting induces long range motions shown in figure 6a. The drop readily deforms its free surface during its translation into the region with lower energy. The competition between the interfacial energy and the local energy determines the morphology of the translating drop. The variation of the curvature along the drop contour decreases with λ due to the increasing influence of the interfacial energy. Figure 7 shows the efficiency of the biharmonic modified scheme is relatively independent of the strength of the local energy.

The boundary integral method developed by [37] has been quite successful in simulating the long time evolution of free boundary fluid problems in a Hele-Shaw cell. However, simulating drops that undergo topological changes remains a complicated, if not ad hoc, process for methods based on sharp interfaces. The diffuse

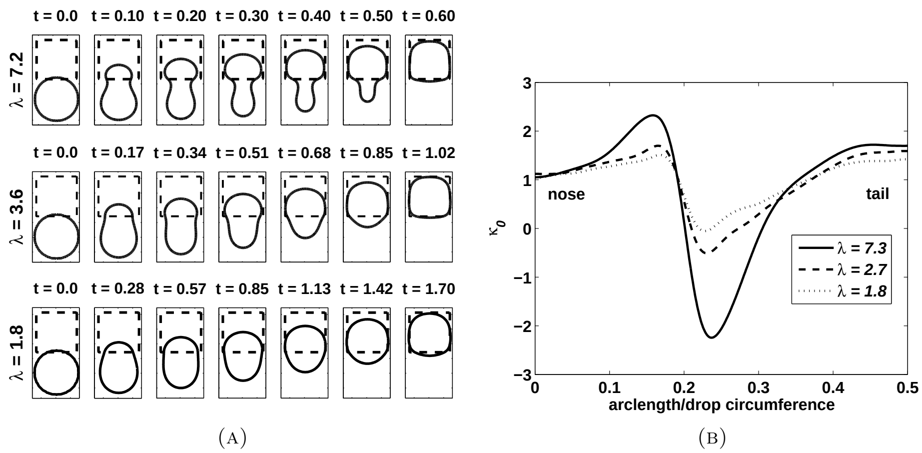

Figure 6. (a) Translation of a Hele-Shaw drop by the electrowetting energy confined in the dashed square. (b) Curvature variations of moving drops at the same center of mass location.

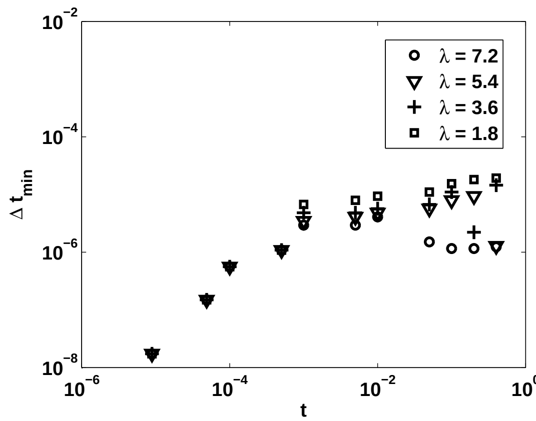

Figure 7. Minimum timestep taken during the simulations with different λ.

interface model naturally handles topology changes such as a drop splitting shown in figure 8. The simulation reproduces the dynamics of the bulk fluid through a gradient flow that monotonically dissipates the energy functional as shown in figure 9. It could be interesting to develop a multi-scale scheme to progressively refine the resolution of the diffuse interface model in the pinch-off region.

5. **Conclusions.** In summary, we have presented some basic analysis of a biharmonic-modified forward difference scheme for a class of fourth order degenerate diffusion equations, that include a possible second order (stable or unstable) term. The analysis assumes that the PDE has a smooth positive solution and that a solution of the scheme can be found to satisfy pointwise upper and lower bound

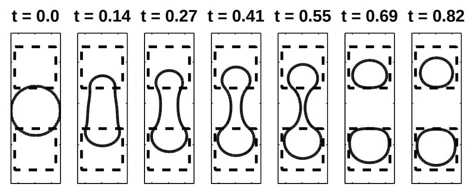

(A)

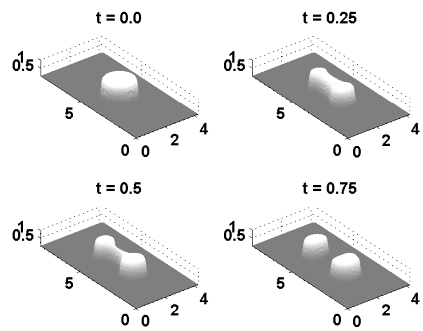

(B)

FIGURE 8. (a) The splitting of a Hele-Shaw drop by two local energies in the dashed squares with $\lambda = 3.6$. (b) The 3 dimensional view of the phase field variables.

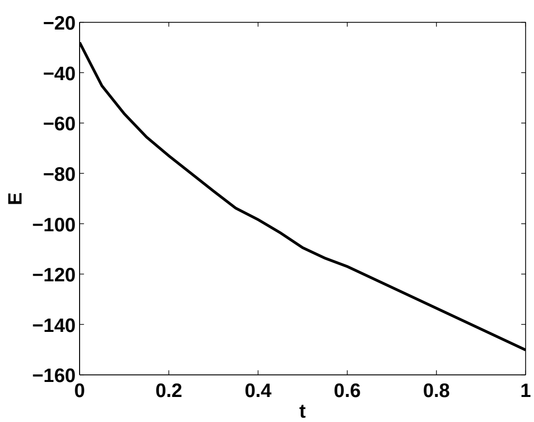

FIGURE 9. Monotonic decrease of the energy functional during the drop splitting.

estimates. Numerical simulations are presented, for a variety of problems, that illustrate that such assumptions are practical and that the class of schemes is both simple to implement and relatively efficient for the tasks at hand. Some complex, real-world examples are presented including a model for electrowetting on dielectric and for coarsening dynamics of a large system of droplets.

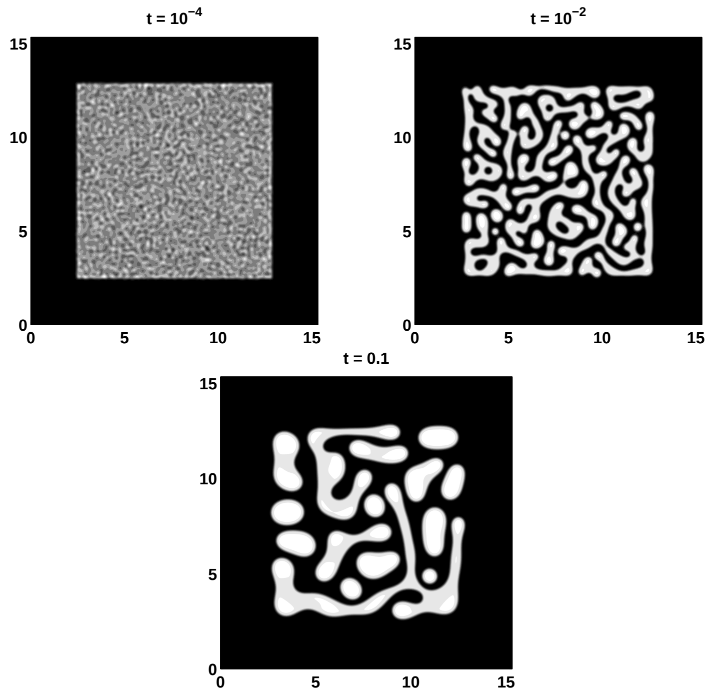

FIGURE 10. Simulation of coarsening from a uniformly distributed random initial condition.

The scheme presented here is related to convex splitting schemes, which have been used for other applications involving higher order equations. A related analysis of such methods for higher order equations for image inpainting is discussed in [45].

Appendix: Modified equation. Consider the finite difference approximation of the nonlinear diffusion (4.5) in one dimension.

$$\frac{u_i^{n+1}-u_i^n}{\Delta t}+M\left(\delta_{xxxx}u^{n+1}-\delta_{xxxx}u^n\right)=-\delta_x\left(u_i^n\delta_x\delta_{xx}u_i^n\right), \tag{5.1}$$

where common central difference operators are used to simplify the formula.

$$\begin{aligned}\delta_x u_i &= \left(u_{i+1/2}-u_{i-1/2}\right)/\Delta x,\\ \delta_x\delta_{xx}u_{i+1/2} &= \left(u_{i+2}-3u_{i+1}+3u_i-u_{i-1}\right)/\Delta x^3,\\ \delta_{xxxx}u_i &= \left(u_{i+2}-4u_{i+1}+6u_i-4u_{i-1}+u_{i-2}\right)/\Delta x^4.\end{aligned}$$

Expanding each terms in the difference equation by Taylor series gives

$$\begin{aligned}\frac{u_i^{n+1}-u_i^n}{\Delta t} &= u_t+\frac{\Delta t}{2}u_{tt}+O\left(\Delta t^2\right),\\ \delta_x\left(u_i^n\delta_x\delta_x x u_i^n\right) &= \left(uu_{xxx}\right)+O\left(\Delta x^2\right),\\ \delta_{xxxx}u^{n+1}-\delta_{xxxx}u^n &= \Delta t u_{xxxxt}+O\left(\Delta t\Delta x^2\right).\end{aligned}$$

Substitute back into the difference equation results the modified equation

$$u_t+\left(uu_{xxx}\right)_x=-\frac{\Delta t}{2}u_{tt}-Mu_{xxxxt}\Delta t+O\left(\Delta x^2+\Delta t^2\right). \tag{5.2}$$

Defining $\mathcal{F}(u) = uu_{xxx}$, we use the fact that

$$u_t = -\mathcal{F}_x + O(\Delta t + \Delta x^2)$$

to remove the time derivatives on the left hand side of (5.2) and obtain

$$u_t + (\mathcal{F}(u))_x = -\Delta t \left[\left(\frac{\partial \mathcal{F}}{\partial u} (\mathcal{F}(u))_x \right)_x - M (\mathcal{F}(u))_{xxxxx} \right] + O\left(\Delta x^2 + \Delta t^2\right)$$

Acknowledgments. We thank Karl Glasner and Tom Beale for useful discussions.

REFERENCES

[1] J. W. Barrett and J. F. Blowey, *Finite element approximation of a model for phase seperation of muti-component alloy with non-smooth free energy*. Numer. Math., **77** (1997), 1–34.

[2] J. W. Barrett and J. F. Blowey, *Finite element approximation of a model for phase separation of a multi-component alloy with a concentration-dependent mobility matrix*, IMA Journal of Numerical Analysis, **18** (1998), 287–328.

[3] J. W. Barrett and J. F. Blowey, *Finite element approximation of a model for phase separation of a multi-component alloy with nonsmooth free energy and a concentration dependent mobility matrix*, Math. Models Methods Appl. Sci., **9** (1999), 627–663.

[4] J. W. Barrett and J. F. Blowey, *Finite element approximation of the Cahn-Hilliard equation with concentration dependent mobility*, Mathematics of Computation, **68** (1999), 487–517.

[5] J. W. Barrett, J. F. Blowey and H. Garcke, *Finite element approximation of a fourth order nonlinear degenerate parabolic equation*, Numer. Math., **80** (1998), 525–556.

[6] J. W. Barrett, J. F. Blowey and H. Garcke, *Finite element approximation of the Cahn-Hilliard equation with degenerate mobility*, SIAM J. Num. Anal., **37** (1999), 286–318.

[7] F. Bernis and A. Friedman, *Higher order nonlinear degenerate parabolic equations*, J. Diff. Equations, **83** (1990), 179–206.

[8] A. L. Bertozzi and M. C. Pugh, *Long-wave instabilities and saturation in thin film equations*, Comm. Pure Appl. Math., **51** (1998), 625–666.

[9] A. L. Bertozzi and M. Pugh, *The lubrication approximation for thin viscous films: Regularity and long time behavior of weak solutions*, Comm. Pur. Appl. Math., **49** (1996), 85–123.

[10] A. Bertozzi and M. Pugh, *Finite-time blow-up of solutions of some long-wave unstable thin film equations*, Indiana Univ. Math. J., **32** (2000), 1323–1366.

[11] A. L. Bertozzi, *The mathematics of moving contact lines in thin liquid films*, Notices of the American Math. Soc., **45** (1998), 689–697.

[12] A. L. Bertozzi, M. P. Brenner, T. F. Dupont and L. P. Kadanoff, *Singularities and similarities in interface flow*, in "Trends and Perspectives in Applied Mathematics" (L. Sirovich, editor), volume **100** of Applied Mathematical Sciences, Springer–Verlag, New York, (1994), 155–208.

[13] A. L. Bertozzi, G. Grün and T. P. Witelski, *Dewetting films: bifurcations and concentrations*, Nonlinearity, **14** (2001), 1569–1592.

[14] M. Brenner and A. Bertozzi, *Spreading of droplets on a solid surface*, Phys. Rev. Lett., **71** (1993), 593–596.

[15] P. Constantin, T. F. Dupont, R. E. Goldstein, L. P. Kadanoff, M. J. Shelley and S.-M. Zhou, *Droplet breakup in a model of the Hele-Shaw cell*, Physical Review E, **47** (1993), 4169–418.

[16] J. Douglas, Jr. and T. Dupont, *Alternating-direction Galerkin methods on rectangles*, in "Numerical Solution of Partial Differential Equations, II (SYNSPADE 1970) (Proc. Sympos., Univ. of Maryland, College Park, Md., 1970)," Academic Press, New York, (1971), 133–214.

[17] T. F. Dupont, R. E. Goldstein, L. P. Kadanoff and Su-Min Zhou, *Finite–time singularity formation in Hele Shaw systems*, Physical Review E, **47** (1993), 4182–4196.

[18] P. Ehrhard and S. H. Davis, *Non-isothermal spreading of liquid drops on horizontal plates*, J. Fluid. Mech., **229** (1991), 365–388.

[19] C. M. Elliott and A. M. Stuart, *The global dynamics of discrete semilinear parabolic equations*, SIAM J. Numer. Anal., **30** (1993), 1622–1663.

[20] C. M. Elliott and H. Garke, *On the cahn hilliard equation with degenerate mobility*, SIAM J. Math. Anal., **27** (1996), 404–423.

[21] D. Eyre, *An unconditionally stable one-step scheme for gradient systems*, Unpublished paper, June 9, 1998.

[22] R. Ferreira and F. Bernis, *Source-type solutions to thin-film equations in higher dimensions*, Euro. J. Appl. Math., **9** (1997), 507–524.

[23] K. Glasner, *Nonlinear preconditioning for diffuse interfaces*, J. Comp. Phys., **174** (2001), 695–71.

[24] K. B. Glasner and T. P. Witelski, *Coarsening dynamics of dewetting films*, Phys. Rev. E, **67** (2003), 016302.

[25] K. Glasner, *A diffuse interface approach to Hele-Shaw flow*, Nonlinearity, **16** (2003), 49–66.

[26] K. B. Glasner and T. P. Witelski, *Coarsening dynamics of dewetting films*, Phys. Rev. E, **67** (2003), 016302.

[27] R. E. Goldstein, A. I. Pesci and M. J. Shelley, *Topology transitions and singularities in viscous flows*, Physical Review Letters, **70** (1993), 3043–3046.

[28] R. E. Goldstein, A. I. Pesci and M. J. Shelley, *An attracting manifold for a viscous topology transition*, Physical Review Letters, **75** (1995), 3665–3668.

[29] H. P. Greenspan, *On the motion of a small viscous droplet that wets a surface*, J. Fluid Mech., **84** (1978), 125–143.

[30] H. P. Greenspan and B. M. McCay, *On the wetting of a surface by a very viscous fluid*, Studies in Applied Math., **64** (1981), 95–112.

[31] J. Greer, A. Bertozzi and G. Sapiro, *Fourth order partial differential equations on general geometries*, J. Computational Physics, **216** (2006), 216–246.

[32] G. Grün and M. Rumpf, *Nonnegativity preserving convergent schemes for the thin film equation*, Num. Math., **87** (2000), 113–152.

[33] L. M. Hocking, *A moving fluid interface on a rough surface*, Journal of Fluid Mechanics, **76** (1976), 801–817.

[34] L. M. Hocking, *A moving fluid interface. Part 2. The removal of the force singularity by a slip flow*, Journal of Fluid Mechanics, **79** (1977), 209–229.

[35] L. M. Hocking, *Sliding and spreading of thin two-dimensional drops*, Q. J. Mech. Appl. Math., **34** (1981), 37–55.

[36] L. M. Hocking, *Rival contact-angle models and the spreading of drops*, J. Fluid. Mech., **239** (1992), 671–68.

[37] T. Hou, J. S. Lowengrub and M. J. Shelly, *Removing the stiffness from interfacial flow with surface-tension*, J. Comp. Phys., **114** (1994), 312–338.

[38] M. G. Lippman, *Relations entre les phènoménes électriques et capillaires*, Ann. Chim. Phys., **5** (1875), 494–548.

[39] H. W. Lu, K. Glasner, C. J. Kim and A. L. Bertozzi, *A diffuse interface model for electrowetting droplets in a Hele-Shaw cell*, Journal of Fluid Mechanics, **590** (2007), 411–435.

[40] J. A. Moriarty, L. W. Schwartz and E. O Tuck, *Unsteady spreading of thin liquid films with small surface tension*, Phys. Fluids A, **3** (1991), 733–742.

[41] T. G. Myers, *Thin films with high surface tension*, SIAM Rev., **40** (1998), 441–462 (electronic).

[42] P. Neogi and C. A. Miller, *Spreading kinetics of a drop on a smooth solid surface*, J. Colloid Interface Sci., **86** (1982), 525–538.

[43] A. Oron, S. H. Davis and S. George Bankoff, *Long-scale evolution of thin liquid films*, Rev. Mod. Phys., **69** (1997), 931–980.

[44] W. H. Press, S. A. Teukolsky, W. T. Vetterling and B. P. Flannery, "Numerical Recipes in C," Second Edition, Cambridge University Press, New York, 1993.

[45] C.-B. Schoenlieb and A. Bertozzi, *Unconditionally stable schemes for higher order inpainting*, 2010.

[46] M. J. Shelley, R. E. Goldstein and A. I. Pesci, *Topological transitions in Hele-Shaw flow*, in "Singularities in Fluids, Plasmas, and Optics" (R. E. Caflisch and G. C. Papanicolaou, editors), Kluwer Academic Publishers, The Netherlands, (1993), 167–188.

[47] P. Smereka, *Semi-implicit level set methods for curvature flow and for motion by surface diffusion*, J. Sci. Comp., **19** (2003), 439–456.

[48] S. M. Troian, E. Herbolzheimer, S. A. Safran and J. F. Joanny, *Fingering instabilities of driven spreading films*, Europhys. Lett., **10** (1989), 25–30.

[49] B. P. Vollmayr-Lee and A. D. Rutenberg, *Fast and accurate coarsening simulation with an unconditionally stable time step*, Physical Review E, **68** (2003), 1–13.

[50] T. P. Witelski and M. Bowen, *Adi methods for high order parabolic equations*, Appl. Num. Anal., **45** (2003), 331–35.
[51] T. P. Witelski, *Equilibrium solutions of a degenerate singular Cahn-Hilliard equation*, Applied Mathematics Letters, **11** (1998), 127–133.
[52] L. Zhornitskaya and A. L. Bertozzi, *Positivity-preserving numerical schemes for lubrication-type equations*, SIAM J. Numer. Anal., **37** (2000), 523–555 (electronic).

Received December 2009; revised July 2010.

E-mail address: bertozzi@math.ucla.edu
E-mail address: ningju@math.okstate.edu
E-mail address: hwlu@mailbox-01.hmc.edu